International Congress Series 1274 (2004) 64–74

www.ics-elsevier.com

Elasticity imaging of atheroma with transcutaneous ultrasound both in longitudinal-axis and short-axis planes

Hiroshi Kanai*, Hideyuki Hasegawa, Nozomi Nakagawa

Graduate School of Engineering, Tohoku University, Aoba-ku Aramaki-aza-Aoba 6-6-05, Sendai 980-8579, Japan

Abstract. This paper describes a noninvasive method for evaluating regional viscoelasticity of the arterial wall in which a novel method is applied to measure minute changes in wall thickness caused by the change in internal pressure. (1) By comparing the pathological findings with the elasticity distribution, statistical parameters for lipid and a mixture of smooth muscle and collagen fibers can be determined. By applying the method to the common carotid arteries, thin collagen fiber was clarified and soft inclusion of lipid in plaque was detected. (2) A new beam steering method was proposed to apply the above method to the plane, which is perpendicular to the axis of the artery. (3) For improvement of classification of tissue, a method was proposed to measure viscosity by generating the change in internal pressure using the external actuation from the skin surface, namely remote actuation. These methods offer the potential for detection of plaque vulnerability in a clinical setting.

Keywords: Viscoelasticity of arterial wall; Tissue characterization; Ultrasound; Atherosclerosis

1. Introduction

Rupture of atherosclerotic plaque is probably the most important factor underlying the sudden onset of acute coronary syndrome [1]. Direct characterization of the composition and vulnerability of atherosclerotic plaque, rather than of the angiographic lumen [2], may offer insight into the mechanisms of plaque regression and progression [3,4] and thereby promote evaluation of cholesterol-lowering therapy [5,6] for reduction of

* Corresponding author. Tel.: +81 22 217 7078; fax: +81 22 263 9444.
E-mail address: hkanai@ecei.tohoku.ac.jp (H. Kanai).

0531-5131/
doi:10.1016/j.ics.2004.07.029

cardiovascular events. Magnetic resonance imaging (MRI) and intravascular ultrasonography (IVUS) are promising technologies for directly imaging plaque morphology [7,8]. For the evaluation of dynamic mechanics, arterial elasticity has been determined by measuring pulse wave velocity [9] and rough change in the diameter of the artery [10,11]. However, the mechanical property of plaque cannot be directly determined by these methods because they evaluate average elasticity of the entire circumference. A method to detect the vulnerability of atherosclerotic plaque with sufficient accuracy has not yet been reported. The purpose of the present study was to determine the regional viscoelasticity in the arterial wall using commercially available transcutaneous ultrasound equipment.

2. Methods

2.1. Measurement of change in thickness of the arterial wall

An ultrasonic beam was sequentially scanned at M positions with a linear-type ultrasonic probe of 7 MHz using conventional ultrasound diagnostic equipment (Toshiba SSH-140A), and multiple (N_m+1) points were preset from the luminal surface to the adventitia along the m-th ultrasonic beam (m=1, . . ., M) with constant intervals of h_0=375 μm at a time t_0 just before the ejection period. By dividing the arterial wall into multiple layers, we defined the n-th layer (n=1, . . ., N_m) as being between two contiguous points, n and n+1, along each beam. For measurement of the change in thickness of each of the N_m layers, the instantaneous depth $x_{m,n}(t)$ of the n-th point along the m-th beam was simultaneously tracked by applying the *phased tracking method* [12,13] to the received ultrasound. The minute decrease of several tenths of a micrometer in thickness of the n-th layer, resulting from the arrival of the pressure wave at the beginning of the ejection period, was determined by $\Delta h_{m,n}(t)=x_{m,n+1}(t)-x_{m,n}(t)-h_0$.

In the *phased tracking method*, for calculation of the autocorrelation function between the quadrature-demodulated signals of sequentially received echoes, a minute phase change of about 0.4° caused by movement of the n-th point during the pulse transmission interval ΔT (=200 μs) can be accurately determined by introducing a *constraint*, namely that their waveforms are identical but their phase values change [12,13]. The lowest value of the change in thickness was validated as being about 0.5 μm by expanding a rubber plate in a water tank [14]. Such a minute change in thickness cannot be measured by any other method. This method has already been applied to the in vivo detection of the regional instantaneous displacement and change in thickness, with sufficient reproducibility, in the interventricular septum [12,13,15] and the common carotid arteries [16,17].

2.2. Elasticity estimation

From the ratio of the maximum decrease in thickness during one heartbeat, $\Delta h_{m,n,\max}=\max_t|\Delta h_{m,n}(t)|$, to the initial thickness h_0 of the n-th layer, the maximum deformation of the n-th layer was obtained by $\Delta\varepsilon_{m,n,\max}=\Delta h_{m,n,\max}/h_0$. Because the

deformation was sufficiently small and was in the linear regime, it showed incremental strain in the radial direction. By assuming that the arterial wall is incompressible and that the blood pressure is applied normally to each layer, the elastic modulus of the n-th layer along the m-th beam, $E_{\theta m,n}$, is approximately given by [18]

$$E_{\theta,m,n} \cong \frac{1}{2}\left(\frac{\rho_{m,n,0}}{h_0} + \frac{N_m - n + 1}{N_m}\right)\frac{\Delta_p}{\Delta_{\varepsilon_{m,n,\max}}} \quad (n = 1, \ldots, N_m;\ m = 1, \ldots, M), \tag{1}$$

where $\rho_{m,n,0}$ is the initial inner radius of curvature of the n-th layer along the m-th beam at a time t_0. We assumed that the pressure in the arterial wall decreases linearly with the distance from the intimal side to the adventitia and that the arterial wall is almost isotropic [19].

For the region with a length of 18 mm (M=60) along the axis of the artery, the regional elasticity $E_{\theta m,n}$ was estimated on the cross-sectional image. Because the reflected ultrasound was received at a sampling interval of 100 ns (=75 μm along depth direction) after the quadrature demodulation, we further divided each layer with a thickness of h_0 into five points, shifted the initial depth of each layer by 1/5 of h_0 and applied the above procedure to each depth. Thus, $E_{\theta,m,n}$ was estimated at intervals of 75 μm in the depth direction and 300 μm in the axial direction. Using a silicone rubber tube with two layers set in an artificial circulation system, the accuracy of the measurement of regional elasticity for each layer has already been validated to be about 0.1 MPa [18], that is the error is about 8% of the elasticity value obtained by a separate static pressure–diameter test.

In in vivo experiments before, the surgical extraction of an iliac artery, and in in vitro experiments (described below) after such extraction, the average elasticity was between 0.96 ± 0.48 and 0.89 ± 0.31 MPa, respectively; the difference between them being about 8%. Thus, the slight influence of assaying the artery through the skin was eliminated.

In separate in vivo experiments, when the pressure of the ultrasonic probe on the skin surface of a healthy subject was set as 8.0, 14.0, 33.2, 40.7, 54.5, and 74.3 mmHg, the measured diameter of the same point of the common carotid artery changed as 6.8, 6.8, 6.6, 6.1, 6.0, and 5.4 mm, respectively. For higher pressure, the cross-section of the artery changes from a circular to an oval shape. We confirmed that the measured elasticity is not influenced by the pressure on the ultrasonic probe to the skin surface as long as the pressure is equal to or less than 30 mmHg. In our in vivo experiments, the ultrasonic probe was held on the skin surface at a pressure of 30 mmHg.

2.3. Beam steering for measurement in the short-axis plane

As shown in Fig. 1(a), in the long-axis plane, all ultrasonic beams become perpendicular to the wall by linear scanning. However, only one beam, which passes through the center of the artery, is perpendicular to the short-axis plane. For measurement in the short-axis plane, as shown in Fig. 1(b), the ultrasonic beams are transmitted to the M (=N+1) directions and designed so that each beam passes through the center, O, of the artery. Under such a setting, the ultrasonic beams are always

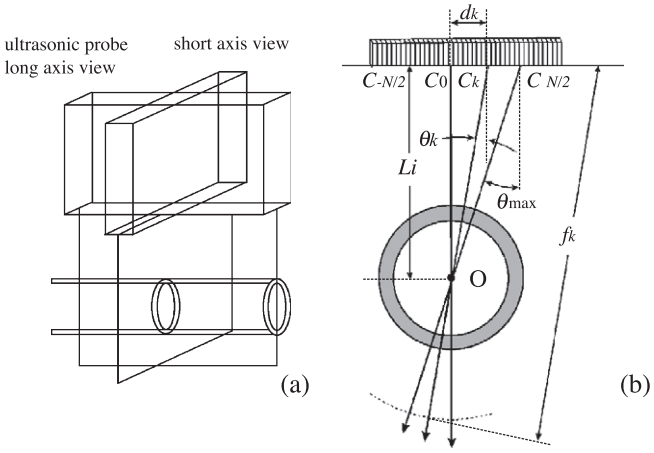

Fig. 1. (a) Illustration of long-and short-axis planes. (b) Schematic diagram of beam steering.

perpendicular to the arterial wall if the cross section of the artery can be assumed a circle. The beam scanning is designed as follows [20]: The distance, d_k, from the center, c_k, of the transmit aperture of the k-th beam (k=−N/2, …, 0, …, N/2) to the center of the probe is expressed as follows:

$$d_k = 0.4\ k\ [\mathrm{mm}]. \tag{2}$$

The beam angle, θ_k, of the k-th beam is expressed as follows:

$$\theta_k = \arctan\frac{d_k}{L_i}\ [\mathrm{rad}], \tag{3}$$

where L_i is the distance from the surface of the probe to the point O. In our system, L_i is variable from 8.5 to 21.5 mm with a pitch of 1 mm (i=1, 2, … , 14). The focal distance of the k-th beam is defined by

$$f_k = \frac{L_i}{\cos\theta_k} + 9\ [\mathrm{mm}]. \tag{4}$$

In Eq. (4), the distance from c_k to O is added by 9 mm so that the focal depth becomes deeper than the posterior wall. The beam width at the posterior wall is widened by this setting, and a wider beam is robust against wall motion, which slips off the beam [21]. By changing the distance, L_i, each ultrasonic beam can be perpendicular to the arterial wall even in the case of subjects with different distances from the skin surface to the artery.

2.4. Viscosity estimation by remote actuation

For assessment of viscosity, changes in blood pressure at multiple frequencies were generated by applying the external cyclic actuation from the skin surface on the brachial artery [22]. Resultant change in blood pressure propagates along the artery and causes change in wall thickness at the carotid artery. In the case of sinusoidal actuation, Eq. (1)

can be rewritten as the complex elastic modulus by replacing Δp and $\Delta\varepsilon_{m,n,\max}$ by $\Delta p_0 e^{j\omega t}$ and $\Delta\varepsilon_{m,n,0}e^{j(\omega t+\varphi)}$ as follows:

$$E^*_{\theta,m,n}(\omega) = \frac{1}{2}\left(\frac{\rho_{m,n,0}}{h_0} + \frac{N_m - n + 1}{N_m}\right)\frac{\Delta p_0}{\Delta\varepsilon_{m,n,0}}e^{j\varphi}, \tag{5}$$

where φ is the phase difference between changes in pressure and wall thickness. Eq. (5) shows that the elastic modulus obtained from the amplitudes, Δp_0 and $\Delta\varepsilon_{m,n,0}$, of changes in blood pressure and strain (change in thickness) corresponds to the absolute value, $|E^*_{\theta,m,n}(\omega)|$, of the complex elastic modulus.

When the Voigt model can be assumed as a viscoelastic model of the wall, the absolute value, $|E^*_{\mathrm{Voigt}}(\omega)|$, of the complex elastic modulus is expressed by the static elastic modulus, E_s, and viscosity constant, η, as follows:

$$|E^*_{Voigt}(\omega)| = \sqrt{E_s^2 + (\omega\eta)^2}. \tag{6}$$

From the in vitro experiments, using extracted human femoral arteries, it was shown that $(\omega\eta)^2/E_s^2 \approx 10$ [23]. Under such a condition, Eq. (6) can be approximated as follows:

$$E^*_{Voigt}(\omega) \approx \omega\eta. \tag{7}$$

From Eq. (7), the viscosity constant, η, can be obtained by estimating the slope of the measured $|E^*_{\theta,m,n}(\omega)|$.

3. Experimental results

3.1. Measurement in the long-axis plane

3.1.1. In vitro determination of statistical parameters

Immediately after nine iliac arteries (25–40 mm in length and 4–24 mm in outer diameter) with plaques extracted from patients with embolism, cross-sectional elasticity distribution, $E_{\theta,m,n}$, was measured using the above method (Fig. 2(a)) under the same artificial circulation system to generate a change in pressure so that it ranged from the diastolic pressure to the systolic pressure of the subjects. After each in vitro measurement, elastica–Masson stain was applied. (Two typical results are shown in Fig. 2(b).) From the stain images, 10 regions with either lipid or a mixture of smooth muscle and collagen fiber were assigned in $E_{\theta,m,n}$ of the nine specimens. (Each histogram of $E_{\theta,m,n}$ in the respective regions is shown in Fig. 2(c).) For the respective categories of the nine arteries, the average and the standard deviation in elasticity were determined to be 81 ± 40 kPa and 1.0 ± 0.63 MPa, which were registered as the reference parameters (Fig. 2(d)).

Based on these reference parameters, each point in the cross-sectional elasticity distribution, which had been noninvasively measured by the above method in separate in vivo experiments, was statistically classified as one of three categories (lipid, mixture of smooth muscle and collagen fiber, or others). Thus, the arterial wall and the atherosclerotic plaque were electronically stained [17].

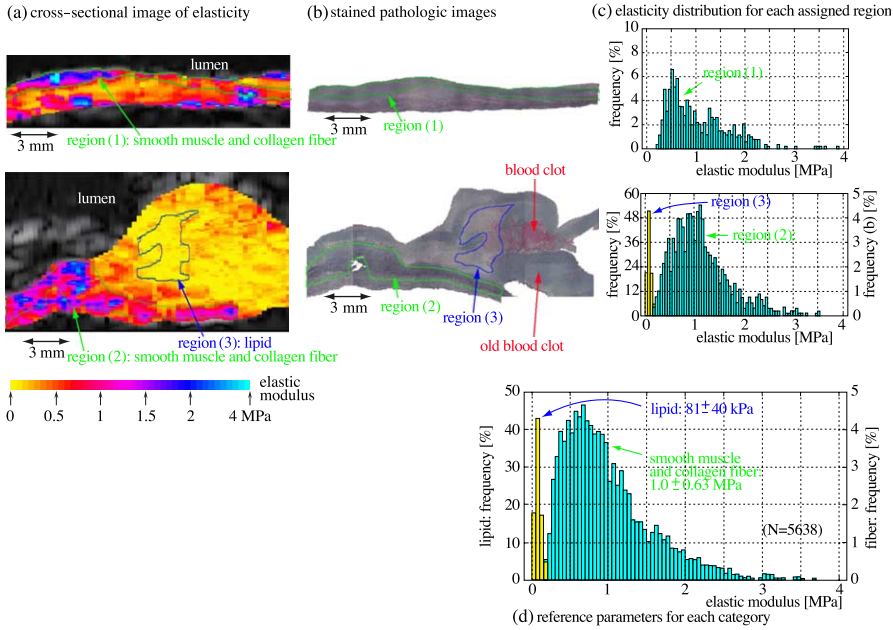

Fig. 2. By referring to the stained image (b), the regions of lipid and of the mixture of smooth muscle and collagen fiber were assigned in the spatial distribution of elasticity $E_{\theta,m,n}$ measured in in vitro experiments (a). From the histogram of $E_{\theta,m,n}$ for each region (c), the elasticity for each category was registered as a reference (d), from which each tissue was categorized as belonging to one of the three categories [17].

3.1.2. In vivo measurement at common carotid arteries

The proposed method was applied to in vivo measurements of the common carotid arteries of a healthy subject (Fig. 3(a)) and a patient with hyperlipidemia having atherosclerotic plaque (Fig. 3(b)). In Fig. 3, for each subject, a cross-sectional image obtained by conventional ultrasound diagnostic equipment is shown at the top. The cross-sectional elasticity distribution of $E_{\theta,\mathrm{m,n}}$ was color-coded and superimposed on the reconstructed B-mode image as shown in the middle. Finally, at the bottom, the categorized result is shown. The lipid and the mixture of smooth muscle and collagen fiber are shown by yellow and cyan, respectively, and the category of "other" is not colored.

3.2. In vivo measurement at common carotid artery in the short-axis plane

The change in the thickness of a common human carotid artery of a 29-year-old male was measured in the short-axis plane. The B-mode image measured by the linear-type probe is shown in Fig. 4. The B-mode images were drawn at the time of the R-wave of the electrocardiogram. Figs. 4(a) and (b) show B-mode images measured by the conventional linear scanning method and the proposed method, respectively. In this experiment, L_i=15.5 mm and the largest beam angle, $\theta_{\max}$, was 21.2°. In Fig. 4, beams at positions l_1 and l_2 measured the same regions of the posterior wall, as measured by beams at the positions, l_1' and l_2'.

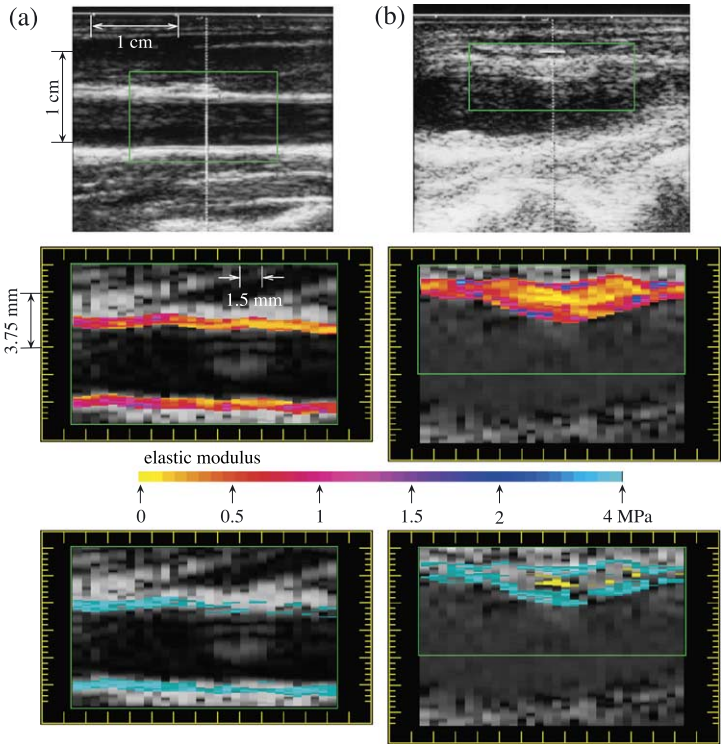

Fig. 3. Common carotid arteries of (a) a healthy male subject (24-year-old) and (b) a male patient with hyperlipidemia (71-year-old). The area outlined by green in each uppermost figure was analyzed in the middle and bottom of the figure [17].

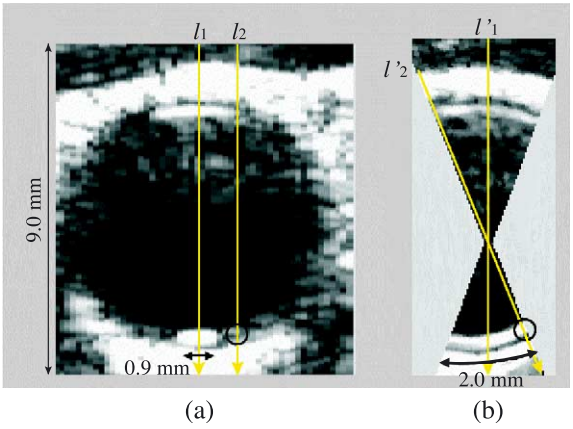

Fig. 4. B-mode images measured by the conventional linear scanning method (a) and the proposed method (b).

M-mode images, electrocardiograms, velocities at the intimal side and the adventitial side of the posterior wall, and changes in wall thickness measured at beam positions l_1, l_2, l'_1 and l'_2 in Figs. 4(a) and (b) are shown in Figs. 5(a), (b), (c) and (d), respectively. By linear scanning, as shown in Fig. 5(a-5), the change in thickness was measured with high reproducibility at the beam position l_1, where the ultrasonic beam was perpendicular to the arterial wall. However, at the beam position l_2 (Fig. 5(b-5)), where the ultrasonic beam was not perpendicular to the arterial wall, the amplitude of the change in thickness was different from that measured at l_1 because the direction of wall expansion due to the heartbeat slipped off the beam. Moreover, the reproducibility during heartbeats was made worse by the decrease in the signal-to-noise ratio of the reflected ultrasonic waves. The ratio, $A(l_2)/A(l_1)$, of amplitudes $A(l_1)$ and $A(l_2)$ of echoes at the beam positions l_1 and l_2 in Fig. 4(a) was 0.059.

As shown in Figs. 5(c-5) and (d-5), using the proposed method, the changes in the thickness of the arterial wall caused by the heartbeat were measured with a similar amplitude, waveform, and high reproducibility at both beam positions l'_1 and l'_2. The ratio

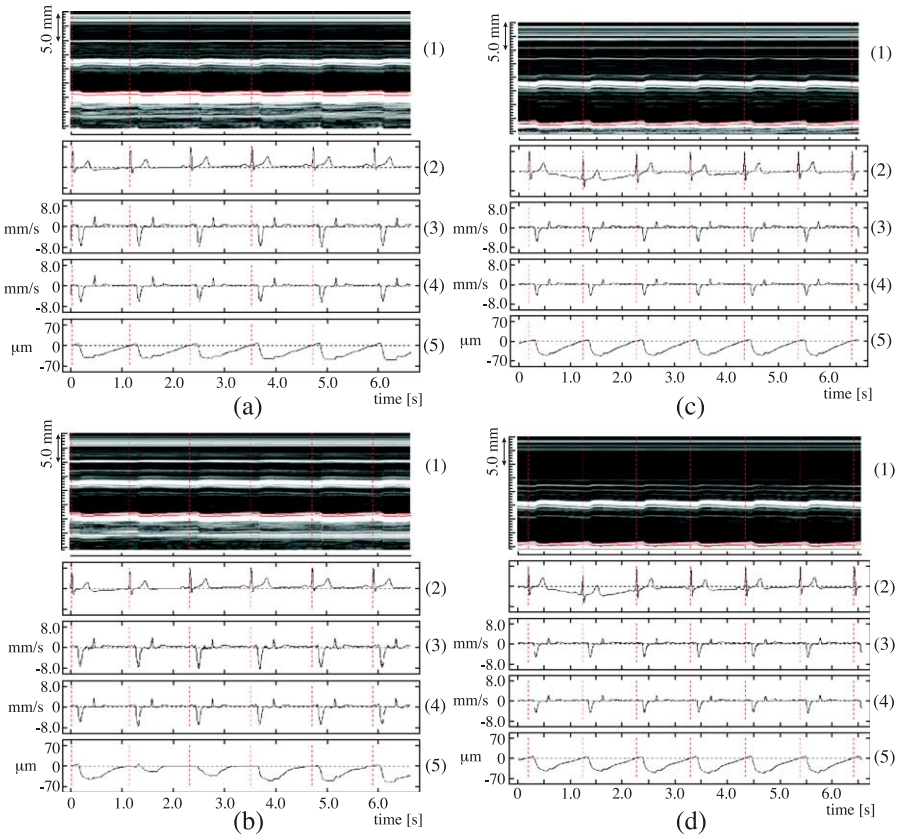

Fig. 5. In vivo experimental results obtained by the linear scanning method at beam positions l_1 (a) and l_2 (b) and by the proposed method at beam positions l'_1 (c) and l'_2 (d). (1) M-mode image. (2) Electrocardiogram. (3) Velocity on intima. (4) Velocity on adventitia. (5) Change in thickness of the posterior wall.

$A(l_2')/A(l_1')$ was 0.92. At the beam position l_2', a beam cannot be scanned to be perpendicular to the wall by the linear scanning method.

Figs. 6(a) and (b) shows the B-mode images of the carotid artery obtained by conventional linear scanning at two different angles. The regions shown by the yellow dotted lines and red dotted lines in Fig. 6(a) correspond to those shown in Fig. 6(b). Figs. 6(c) and (d) shows the cross-sectional images of elastic modulus measured in two different regions, shown by yellow dotted lines and red dotted lines in Figs. 6(a) and (b), respectively. Figs. 6(c) and (d) was measured at the same angles as Figs. 6(a) and (b), respectively. The elastic modulus is obtained by the maximum change in thickness and the pulse pressure measured at the upper arm. The resolution of the cross-sectional image of elastic modulus was 80 μm in the depth direction and $1.43^\circ \pm 0.5^\circ$ in the circumferential direction.

The region of the carotid artery between two red dotted lines in Fig. 6(b) was measured. Then the probe was rotated about 20° along the neck, and the region between two yellow dotted lines in Fig. 6(a) was measured. It is recognized that the elasticity images of the regions between two green dotted lines shown in Figs. 6(c) and (d), which are measured by both measurements, correspond to each other. The mean value and the standard deviation of the measured elastic modulus shown in Figs. 6(c) and (d) were 0.18 ± 0.14 and 0.2 ± 0.15 MPa, respectively.

From these results, using the proposed method, the elasticity distribution of the arterial wall can be measured transcutaneously within the wide region in the short-axis plane.

3.3. In vivo viscosity measurement at common carotid artery

Fig. 7(a-1) shows the M-mode image of a human carotid artery of a 30-year-old male. Fig. 7(a-3) shows the blood pressure measured at the radial artery with an applanation tonometer. By setting two points, A (intimal side) and B (adventitial side), along an ultrasonic beam at the R-wave of electrocardiogram, the velocities, $v_A(t)$ and $v_B(t)$, of these points were obtained by the *phased tracking method* as shown in Figs. 7(a-4) and (a-5).

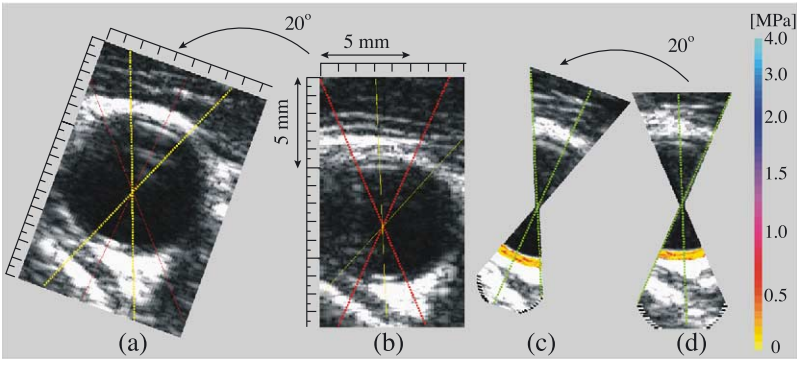

Fig. 6. (a) and (b) are B-mode images of the carotid artery in the short-axis plane obtained by the conventional linear scanning method. (c) Cross-sectional elasticity image measured from the direction shown with yellow lines in (a). (d) Cross-sectional elasticity image measured from the direction shown with red lines in (b).

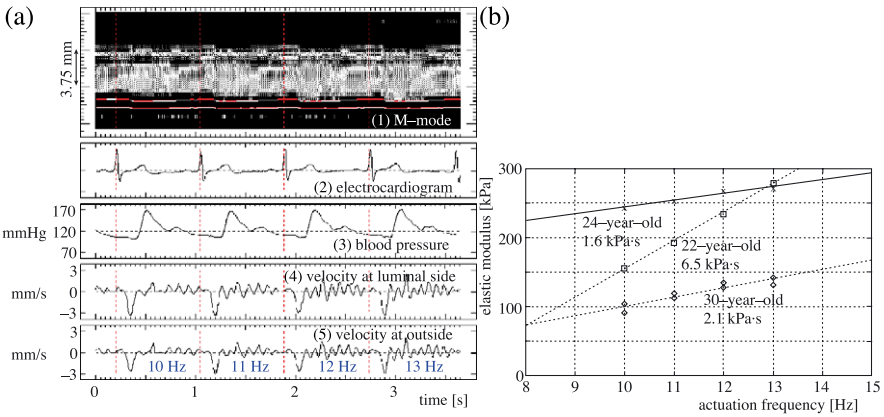

Fig. 7. (a) (1) M-mode image. (2) Electrocardiogram. (3) Blood pressure. (4) Velocity at intimal side. (5) Velocity at adventitial side. (b) Absolute value of complex elastic modulus plotted as a function of actuation frequency.

In Figs. 7(a-4) and (a-5), it is found that there are velocity components caused by remote actuation at each actuation frequency.

In systole, there are velocity components caused by the heartbeat, and it is difficult to discriminate components caused by remote actuation from those caused by the heartbeat. Therefore, the amplitude of velocity components caused by remote actuation is measured in diastole by applying Fourier transform with a Hanning window at 0.5 s after R-wave of the electrocardiogram. From the estimated amplitudes of the change in internal pressure and the change in wall thickness, the absolute value of complex elastic modulus at each actuation frequency was obtained based on Eq. (5) (in this experiment, $M=N_m=1$) and was plotted as a function of actuation frequency as shown in Fig. 7(b). In Fig. 7(b), it is found that the absolute values of elastic modulus for three subjects increase with actuation frequency. The viscosity constants were estimated to be 2.1 kPa · s (30-year-old male), 6.5 kPa · s (22-year-old male), and 1.6 kPa · s (24-year-old male), respectively, and the order of these values was the same as those reported in the literature (about 5 kPa · s) [24].

4. Conclusion

In this study, the regional viscoelasticity of the arterial wall was measured with transcutaneous ultrasound. This novel approach offers potential for the diagnosis of the vulnerability of plaque in a clinical setting.

References

[1] P.R. Moreno, et al., Macrophage infiltration in acute coronary syndromes. Implication for plaque rupture, Circulation 90 (1994) 775–778.

[2] W.C. Little, et al., Can coronary angiography predict the site of a subsequent myocardial infarction in patients with mild-to-moderate coronary artery disease? Circulation 78 (1988) 1157–1166.

[3] H.M. Loree, et al., Effects of fibrous cap thickness on peak circumferential stress in model atherosclerotic vessels, Circ. Res. 71 (1992) 850–858.
[4] E. Falk, et al., Coronary plaque disruption, Circulation 92 (1995) 657–671.
[5] G. Brown, et al., Regression of coronary artery disease as a result of intensive lipid-lowering therapy in men with high levels of apolipoprotein B, N. Engl. J. Med. 323 (1990) 1289–1298.
[6] J. Shepherd, et al., Prevention of coronary heart disease with pravastatin in men with hypercholesterolemia, N. Engl. J. Med. 333 (1995) 1301–1307.
[7] M.V. McConnell, et al., MRI of rabbit atherosclerosis in response to dietary cholesterol lowering, Arterioscler. Thromb. Vasc. Biol. 19 (1999) 1956–1959.
[8] B.N. Potkin, et al., Coronary artery imaging with intravascular high-frequency ultrasound, Circulation 81 (1990) 1575–1585.
[9] P. Hallock, Arterial elasticity in man in relation to age as evaluated by the pulse wave velocity method, Arch. Int. Med. 54 (1934) 770–798.
[10] R.H. Peterson, R.E. Jensen, R. Parnell, Mechanical properties of arteries in vivo, Circ. Res. 8 (1960) 622–639.
[11] F. Hansen, et al., Diameter and compliance in the human common carotid artery—variations with age and sex, Ultrasound Med. Biol. 21 (1995) 1–9.
[12] H. Kanai, et al., Transcutaneous measurement and spectrum analysis of heart wall vibrations, IEEE Trans. UFFC 43 (1996) 791–810.
[13] H. Kanai, et al., Noninvasive evaluation of local myocardial thickening and its color-coded imaging, IEEE Trans. UFFC 44 (1997) 752–768.
[14] H. Kanai, et al., Accuracy evaluation in ultrasonic-based measurement of microscopic change in thickness, Electron. Lett. 35 (1999) 949–950.
[15] H. Kanai, Y. Koiwa, Myocardial rapid velocity distribution, Ultrasound Med. Biol. 27 (2001) 481–498.
[16] H. Kanai, Y. Koiwa, J. Zhang, Real-time measurements of local myocardium motion and arterial wall thickening, IEEE Trans. UFFC 46 (1999) 1229–1241.
[17] H. Kanai, et al., Elasticity imaging of atheroma with transcutaneous ultrasound—preliminary study, Circulation 107 (2003) 3018–3021.
[18] H. Hasegawa, et al., A method for evaluation of regional elasticity of the arterial wall with non-uniform wall thickness by measurement of its change in thickness during an entire heartbeat, 2000 IEEE Ultrason Symp. Proc. (2000) pp. 1829–1832.
[19] D.J. Patel, et al., Dynamic anisotropic viscoelastic properties of the aorta in living dogs, Circ. Res. 32 (1973) 93–107.
[20] N. Nakagawa, H. Hasegawa, H. Kanai, Cross-sectional elasticity imaging of carotid arterial wall in short-axis plane by transcutaneous ultrasound, Jpn. J. Appl. Phys. 43 (2004) 3220–3226.
[21] M. Watanabe, H. Kanai, Optimization of focal position of ultrasonic beam in measurement of small change in arterial wall thickness, Jpn. J. Appl. Phys. 40 (2001) 3918–3921.
[22] H. Hasegawa, H. Kanai, Measurement of elastic moduli of the arterial wall at multiple frequencies by remote actuation for assessment of viscoelasticity, Jpn. J. Appl. Phys. 43 (2004) 3197–3203.
[23] H. Hasegawa, H. Kanai, Measurement of change in wall thickness of cylindrical shell at multiple frequencies caused by remote actuation for assessment of regional viscoelasticity of arterial wall, Proc. Intern'l. Congr. Acoust. (2004) I469–I472.
[24] B.M. Learoyd, M.G. Taylor, Alterations with age in the viscoelastic properties of human arterial walls, Circ. Res. 18 (1966) 278–292.